Understanding Helical Magnetic Dynamo Spectra with a Nonlinear Four-Scale Theory

Eric G. Blackman
Department of Physics &Astronomy and Laboratory for Laser Energetics, University of Rochester, Rochester NY 14627; email: blackman@pas.rochester.edu
(submitted to MNRAS)

ABSTRACT

Recent MHD dynamo simulations for magnetic Prandtl number > 1 demonstrate that when MHD turbulence is forced with sufficient kinetic helicity, the saturated magnetic energy spectrum evolves from having a single peak below the forcing scale to become doubly peaked with one peak at the system (=largest) scale and one at the forcing scale. The system scale field growth is well modeled by a recent nonlinear two-scale nonlinear helical dynamo theory in which the system and forcing scales carry magnetic helicity of opposite sign. But a two-scale theory cannot model the shift of the small-scale peak toward the forcing scale. Here I develop a four-scale helical dynamo theory which shows that the small-scale helical magnetic energy first saturates at very small scales, but then successively saturates at larger values at larger scales, eventually becoming dominated by the forcing scale. The transfer of the small scale peak to the forcing scale is completed by the end of the kinematic growth regime of the large scale field, and does not depend on magnetic Reynolds number R_M for large R_M. The four-scale and two-scale theories subsequently evolve almost identically, and both show significant field growth on the system and forcing scales that is independent of R_M. In the present approach, the helical and nonhelical parts of the spectrum are largely decoupled. Implications for fractionally helical turbulence are discussed.

Key Words: MHD; turbulence; ISM: magnetic fields; galaxies: magnetic fields; stars: magnetic fields; methods: numerical

1. Introduction

Most all ionized astrophysical rotators are turbulent and carry magnetic fields. For astrophysical objects such as the sun, helical dynamo theory was original proposed as a

theory to model the large scale field generation on scales larger than that of the driving turbulence (e.g. Parker 1955; Steenbeck, Krause, Rädler 1966; Moffatt 1978; Parker 1979). Also of interest is to understand the *overall* shape and amplitude of the magnetic energy spectrum from helical or nonhelical dynamo action on both large and small scales (e.g. Pouquet, Frisch, Leorat 1976, Kulsrud & Anderson 1992, Brandenburg et al. 1995; Hawley, Gammie, Balbus 1995,1996; Brandenburg 2001, Shekochihin et al. 2002ab, Maron & Cowley 2002; Maron & Blackman 2002). When the effect of the growing magnetic field on the turbulent velocity is ignored, the dynamo model is kinematic. We know that kinematic theory is incomplete since the dynamo must represent a solution of the full nonlinear magnetohydrodynamic (MHD) equations. In this context, much of theoretical dynamo research can be divided into two categories: (1) that which focuses on the fundamental principles, with the goal of determining a correct and useful nonlinear theory, and (2) that which parameterizes the backreaction of the growing magnetic field on the turbulent velocities and uses it in the dynamo equations to model the fields of specific objects in detail. This paper falls into the former category.

Turbulence that produces astrophysical dynamos can either arise from external forcing or be self-driven from shear. Examples of the former are supernova driving in the Galaxy (e.g. Ruzmaikin, Shukurov, Sokoloff 1988) or thermal convection driving in the sun (e.g. Parker 1979), and an example of the latter is the magneto-rotational instability (MRI) (Balbus & Hawley 1991;1998). In either forced or self-driven dynamos, there exist both helical or nonhelical varieties. Nonhelical vs. helical refers to the situation in which turbulence has either zero vs. finite pseudoscalar quantities such as the kinetic helicity $\overline{\mathbf{v} \cdot \nabla \times \mathbf{v}}$, where $\mathbf{v}$ is the turbulent velocity, and the overbar represents some volume average (within a given hemisphere for a rotator). Such a correlation can be derived from the statistical tendency for rising (falling) eddies to twist in the opposite (same) sense as the underlying rotation as they expand (contract) and conserve angular momentum in stratified rotator. When kinetic helicity is present, the turbulence can generate a global large scale field (e.g. Moffatt 1978; Parker 1979) whose associated sign of flux lasts many overturn times of the largest turbulent eddy. As discussed in Blackman (2002b), such a global field is not to be confused with fields produced in nonhelical simulations for which the largest turbulent scale is the box scale. In this latter case, magnetic energy will arise on the scale of the box, but the sign of its flux will change every overturn time scale. For example, nonstratified MRI simulations (Hawley, Gammie, Balbus 1995) for which no kinetic helicity is present, produce magnetic energy with maximum azimuthal scale of order the box height, but the turbulence also extends to this scale, and the field does not maintain a coherent flux longer than a large eddy turnover time ($\sim$ an orbit time). In contrast, helical MRI simulations in a non-periodic box (Brandenburg et al. 1995) were shown to incur a helical

dynamo which sustains a large scale flux over many orbit times. This latter type of global field is extremely helpful in producing jets and coronae, since it can survive the buoyant rise without shredding on its way up (Blackman 2003). (Note that Stone et al. (1996) claimed that no helicity was observed in stratified periodic box disk simulations. But they averaged over their entire box to test for helicity, and since the northen and southern hemispheres must produce opposite sign, the box averaged helicity would be expected to vanish.)

As the amplification of magnetic fields and the associated MHD turbulence represent highly nonlinear problems, understanding the backreaction of the magnetic field on the field growth itself has been an evolving topic of study (e.g. Piddington 1981, Kleeorin & Ruzmaikin 1982, Vainshtein & Cattaneo 1992, Cattaneo & Hughes 1996, Kulsrud & Anderson 1992, Field, Blackman, Chou 1999, Blackman & Field 2000, Brandenburg 2001, Field & Blackman 2002, Blackman & Field 2002). Some recent developments (Brandenburg 2001; Field & Blackman 2002; Blackman & Field 2002; Brandenburg, Dobler, Subramanian 2002; Blackman & Brandenburg 2002; Maron & Blackman 2002) have emerged from focusing numerically and analytically on the simplest dynamo forced dynamos for which the underlying principles can be identified. Experiments have been performed in which a turbulent velocity spectrum is first established in the absence of magnetic fields in a periodic box and then a weak seed spectrum of magnetic energy is input (e.g. Meneguzzi, Frisch, Pouquet 1981; Kida, Yanase, Mizushima 1991; Brandenburg 2001, Maron & Cowley 2002, Maron & Blackman 2002). The nonlinear evolution the magnetic energy spectrum to saturation can then be studied as the system is driven. (Note that these simulations are distinct from those in which an initial uniform background field is also assumed e.g. Maron & Goldreich 2002; Cho, Lazarian & Vishniac 2002)

The shape of the resulting spectrum depends on the fractional helicity. Define the fractional kinetic helicity $f_h \equiv |\langle \mathbf{v}_f \cdot \nabla \times \mathbf{v}_f \rangle / v_f^2 k_2|$, where $\mathbf{v}_f$ is the turbulent velocity on the forcing scale and k_f is the forcing wavenumber. When forced such that $f_h = 0$, the magnetic spectrum saturates with the magnetic energy seemingly piling up close to the resistive scale for magnetic Prandtl number (the ratio of viscosity to magnetic diffusivity $Pr_M \equiv \nu/\lambda$) > 1, not near the forcing scale (Kida, Yanase, Mizushima 1991; Maron & Cowley 2001; Schekochihin 2002ab). This contradicts, for example, observations of the Galactic magnetic field, which does not seem to have a peak on the resistive scale, (Beck et al. & 1996). On the other hand, recent simulations of Haugen et al. (2003) suggest that the peak may not be at the resistive scale even for $Pr > 1$. Determing the location of the peak for the nonhelical dynamo for $Pr > 1$ is presently an active area of research. All studies seem to at least agree that the peak is below the forcing scale.

By contrast, simulations that force with $f_h \sim 1$ show production of large scale fields at

the box scale and a peak at the forcing scale (Brandenburg 2001). Maron and Blackman (2002) studied what happens to the spectrum both above and below the forcing scale as a function of f_h. By starting with an initial spectrum that represented the saturated state of an $f_h = 0$ simulation, they found that for f_h above a critical value ($= k_1/k_2$, where k_1 is the box scale) a peak at k_1 emerged, and as f_h was further increased toward 1, the peak originally at the sub-forcing scale increasingly depleted. A peak at the forcing scale emerged. The adjusted shape of the spectrum at and below the forcing scale established itself on a kinematic growth time scale of the k_1 field.

The growth rate and saturation value of the large scale field at k_1 is now well understood by a nonlinear two-scale dynamo theory based on magnetic helicity conservation and exchange between the small scale (assumed to be the forcing scale) and the box (large) scale (Field & Blackman 2002; Blackman & Field 2002): Growth of the large scale field corresponds to a growth of large scale magnetic helicity. Magnetic helicity conservation dictates that a small scale helical field must then also grow of the opposite sign. Because the growth driver for the large scale helicity also depends on the small scale magnetic helicity, the growth of the latter ends up quenching the large scale dynamo. But there is an important limitation of the two-scale theory. Why should the growth of the small scale compensating magnetic helicity occur at the forcing scale and not at some much smaller scale? Answering this can help to understand why the small-scale magnetic energy peak initially at sub-forcing scales in simulations of Maron and Blackman (2002) migrates to the forcing scale when sufficient kinetic helicity is input.

To address these questions, I develop a simple four-scale approach which predicts that the small scale magnetic helicity and current helicity grow fastest on the smallest scale on which there is both a finite turbulent velocity and magnetic field. (This would be the viscous scale for $Pr_M \geq 1$ and the resistive scale for $Pr_M \leq 1$.) The magnetic engergy and current helicities saturate fastest at these small scales. Eventually however, larger values are reached at larger scales until the small scale growth is dominated by the forcing scale, essentially justifying a two-scale approach by the time the kinematic growth phase for the k_1 field ends. It is important to emphasize that the mean field formalism herein describes the dynamical evolution of both the large and small scale magnetic and current helicities. The backreaction of the small scale current helicity on the kinetic helicity, and thus on the growth of the large scale field is treated dynamically. We will see that significant growth of the large scale field proceeds unimpeded at early times, but at late times, the backreaction from the small scale field slows the growth to a resistively limited pace. It is imporant to emphasize that the dynamical mean field theory studied herein, albeit a simplified theory, goes beyond the kinematic mean field theory of standard textbooks which does not include the backreaction.

In section 2, the basic role of helicity conservation in large scale dynamo theory is discussed and the four-scale set of equations (3 of which are coupled) are derived. In section 3, the equations are solved. The solutions and their interpretation, discussed in section 4. Section 5 is the conclusion.

2. The Four-scale Nonlinear Dynamo

The mean field dynamo (MFD) theory has been a useful framework for modeling the in situ origin of large-scale magnetic field growth in planets, stars, and galaxies (Moffatt 1978; Parker 1979 Krause & Rädler 1980; Zeldovich, Ruzmaikin, Sokoloff 1983) and has also been invoked and to explain the sustenance of fields in fusion devices (see Ortolani & Schnack 1993; Bellan 2000; Ji & Prager 2002 for reviews). Pouquet, Frisch & Leorat (1976) derived approximate evolution equations for the spectra of kinetic energy, magnetic energy, kinetic helicity, and magnetic helicity and demonstrated the need to consider magnetic helicity in more carefully in the context of dynamo theory. Recent progress in modeling the fully nonlinear dynamical field growth and saturation seen in simulations (Brandenburg 2001) has come from dynamically incorporating magnetic helicity evolution using a two-scale theory (Field & Blackman 2002, Blackman & Brandenburg 2002, Blackman & Field 2002). Previous attempts (Zeldovich, Ruzmaikin, Sokoloff 1983, Kleeorin & Ruzmaikin 1982, Kleeorin, Rogachevskii, Ruzmaikin 1995, Gruzinov & Diamond 1995, Bhattacharjee & Yuan 1995) to use magnetic helicity in dynamo theory did not produce a time dependent dynamical theory.

To develop the new four scale theory and make contact with the previous work, I first average the magnetic induction equation to obtain the basic MFD equation (Moffatt 1978)

$$\partial_t \overline{\mathbf{B}} = \nabla\times\overline{\boldsymbol{\mathcal{E}}} + \nabla\times(\overline{\mathbf{V}}\times\overline{\mathbf{B}}) - \lambda\nabla^2\overline{\mathbf{B}}, \tag{1}$$

where $\overline{\mathbf{B}}$ is the mean (large-scale) magnetic field in Alfvén speed units, $\lambda = \frac{\eta c^2}{4\pi}$ is the magnetic diffusivity in terms of the resistivity η, $\overline{\mathbf{V}}$ is the mean velocity which I set $= 0$, and $\overline{\boldsymbol{\mathcal{E}}} = \langle \mathbf{v}\times\mathbf{b}\rangle$ is the turbulent electromotive force, a correlation between fluctuating velocity $\mathbf{v}$ and magnetic field $\mathbf{b}$ in Alfvén units. Instead of the assuming that there are two scales as in Field & Blackman (2002) and Blackman & Field (2002), here I generalize and assume that there are four scales on which magnetic helicity can reside, such that $k_4 > k_3 > k_2 > k_1 > 0$. An example is to take $k_2 = k_f$, the forcing wavenumber, $k_4 = k_\lambda$, the resistive wavenumber, and $k_3 = k_\nu$ viscous wavenumber. We can interpret $\overline{\mathbf{B}}$, $\overline{\mathbf{A}}$ and $\overline{\boldsymbol{\mathcal{E}}}$ as the mean components of $\mathbf{B}, \mathbf{A}$ and $(\mathbf{v}\times\mathbf{b})$ that varies on a scale k_1^{-1} in a closed system.

The total magnetic helicity, $H = \langle \mathbf{A}\cdot\mathbf{B}\rangle_{vol}$, satisfies (Woltjer 1958; Moffatt 1978 Berger

& Field 1984)

$$\partial_t H = -2\langle \mathbf{E}\cdot\mathbf{B}\rangle_{vol}, \tag{2}$$

where $\mathbf{E} = -\partial_{\mathbf{t}}\mathbf{A} - \nabla\phi$, ϕ is the scalar potential, and $\langle\rangle_{vol}$ indicates a global volume average. Such a conservation formula also applies separately to each scale. That is, using $\overline{\mathbf{E}} = \partial_t\overline{\mathbf{A}} - \nabla\overline{\phi}$, $\mathbf{e}_2 = \partial_t\mathbf{a}_2 - \nabla\phi_2$ and $\mathbf{e}_3 = \partial_t\mathbf{a}_3 - \nabla\phi_3$ and dotting with $\overline{\mathbf{B}}$, $\mathbf{b}_2$ and $\mathbf{b}_3$ respectively we obtain

$$\partial_t H_1 = 2\langle\overline{\boldsymbol{\mathcal{E}}}\cdot\overline{\mathbf{B}}\rangle_{vol} - 2\lambda\langle\overline{\mathbf{J}}\cdot\overline{\mathbf{B}}\rangle_{vol}, \tag{3}$$

$$\partial_t H_2 = -2\langle\mathbf{e}_2\cdot\mathbf{b}_2\rangle_{vol}, \tag{4}$$

$$\partial_t H_3 = -2\langle\mathbf{e}_3\cdot\mathbf{b}_3\rangle_{vol}, \tag{5}$$

and

$$\partial_t H_4 = -2\langle\mathbf{e}_4\cdot\mathbf{b}_4\rangle_{vol}, \tag{6}$$

where $H_1 \equiv \langle\overline{\mathbf{A}}\cdot\overline{\mathbf{B}}\rangle_{vol}$, $H_2 \equiv \langle\mathbf{a}_2\cdot\mathbf{b}_2\rangle_{vol}$, $H_3 \equiv \langle\mathbf{a}_3\cdot\mathbf{b}_3\rangle_{vol}$ and $H_4 \equiv \langle\mathbf{a}_4\cdot\mathbf{b}_4\rangle_{vol}$. I now derive expressions for $\langle\overline{\boldsymbol{\mathcal{E}}}\cdot\overline{\mathbf{B}}\rangle_{vol}$, $\langle\mathbf{e}_2\cdot\mathbf{b}_2\rangle_{vol}$, $\langle\mathbf{e}_3\cdot\mathbf{b}_3\rangle_{vol}$, and $\langle\mathbf{e}_4\cdot\mathbf{b}_4\rangle_{vol}$. I assume that mixed correlations between fluctuating quantities of widely separated scales (which fluctuate on widely different time scales) do not contribute. Thus I ignore terms of the form e.g. $\langle\mathbf{b}_2\cdot\mathbf{j}_3\rangle$. This is an important simplifying assumption which really needs to be tested numerically, and I will come back to it again in section 4. Note however that this assumption is not the same as ignoring the effect of the small scale fields on the large scale field growth, or ignoring the nonlinear backreaction altogether: Eqn. (3-6) along with (8-13) show that nonlinear couplings between disparate scales also occur because the time evolution for the large scale magnetic helicity depends non-linearly on the time evolution of the small scale helicities. These latter couplings are included, even when mixed correlations are not included. We then have

$$\langle\overline{\boldsymbol{\mathcal{E}}}\cdot\overline{\mathbf{B}}\rangle_{vol} = \langle\overline{\boldsymbol{\mathcal{E}}}_2\cdot\overline{\mathbf{B}}\rangle_{vol} + \langle\overline{\boldsymbol{\mathcal{E}}}_3\cdot\overline{\mathbf{B}}\rangle_{vol} \tag{7}$$

where $\overline{\boldsymbol{\mathcal{E}}}_2 = \overline{\mathbf{v}_2\times\mathbf{b}_2}$ and $\overline{\boldsymbol{\mathcal{E}}}_3 = \overline{\mathbf{v}_3\times\mathbf{b}_3}$, and

$$-\langle\mathbf{e}_2\cdot\mathbf{b}_2\rangle_{vol} = -\langle\overline{\boldsymbol{\mathcal{E}}}_2\cdot\overline{\mathbf{B}}\rangle_{vol} + \langle(\mathbf{v}_3\times\mathbf{b}_3)_2\cdot\mathbf{b}_2\rangle_{vol} - \lambda\langle\mathbf{j}_2\cdot\mathbf{b}_2\rangle_{vol} \tag{8}$$

$$-\langle\mathbf{e}_3\cdot\mathbf{b}_3\rangle_{vol} = -\langle(\mathbf{v}_3\times\mathbf{b}_3)_2\cdot\mathbf{b}_2\rangle_{vol} - \langle\overline{\boldsymbol{\mathcal{E}}}_3\cdot\overline{\mathbf{B}}\rangle_{vol} - \lambda\langle\mathbf{j}_3\cdot\mathbf{b}_3\rangle_{vol} \tag{9}$$

and

$$\langle\mathbf{e}_4\cdot\mathbf{b}_4\rangle_{vol} = \lambda\langle\mathbf{j}_4\cdot\mathbf{b}_4\rangle_{vol} \tag{10}$$

where the overbar indicates averages which vary on scales k_1^{-1} wavenumber, the $()_2$ indicates averages which vary on scales $\geq k_2^{-1}$. Eqn. (10) follows because $\mathbf{v}_4 = 0$, as I have assumed k_4 is taken at the resistive scale and that mixed scale correlations vanish.

In what follows I will solve for the nonlinear time evolution of the magnetic helicity at each of the four scales. Blackman & Field (2002) showed that a proper nonlinear theory must technically include the time evolution of $\overline{\boldsymbol{\mathcal{E}}}_2$ and by generalization here, also the time evolution for $\overline{\boldsymbol{\mathcal{E}}}_3$ into the theory. However, they also showed that for the specific case for which triple correlations in $\partial_t \overline{\boldsymbol{\mathcal{E}}}_2$ are treated as damping terms with a damping time $\tau_2 = 1/k_2 v_2$, neglecting the time evolution of the turbulent electromotive force does not qualitatively influence the solution. Adopting this specific case, the implication of their result for the present theory is that

$$\overline{\boldsymbol{\mathcal{E}}}_2 = \frac{\tau_2}{3}(\overline{\mathbf{j}_2 \cdot \mathbf{b}_2} - \overline{\mathbf{v}_2 \cdot \nabla \times \mathbf{v}_2})\overline{\mathbf{B}} - \overline{\beta}_2 \overline{\mathbf{J}}, \tag{11}$$

where β_2 is a diffusivity computed from velocities at the k_2 scale. (The form of the diffusivity is not essential for the present discussion, and I will later scale it to its kinematic value.) Similarly, we also have

$$\overline{\boldsymbol{\mathcal{E}}}_3 = \overline{\mathbf{v}_3 \times \mathbf{b}_3} = \frac{\tau_3}{3}(\overline{\mathbf{j}_3 \cdot \mathbf{b}_3})\overline{\mathbf{B}} - \overline{\beta}_3 \overline{\mathbf{J}}, \tag{12}$$

and

$$(\mathbf{v}_3 \times \mathbf{b}_3)_2 = \frac{\tau_3}{3}(\mathbf{j}_3 \cdot \mathbf{b}_3)_2 \mathbf{b}_2 - (\beta_3)_2 \mathbf{j}_2, \tag{13}$$

where $\tau_3 = 1/k_3 v_3$, and I assume that there are no kinetic helicity contributions at the k_3 scale. This is reasonable because I am focusing on the case in which the kinetic helicity is peaked at the forcing scale, and kinetic helicity does not cascade efficiently. If the k_1 field is maximally helical, the current helicity, magnetic helicity and magnetic energy for the k_1 scale are simply related by powers of k_1. (However, the third term of (8) and the second term of (9) involve a subtly that will be explained below.) Combining equations (6-13) we have

$$\partial_t H_1 = 2\frac{\tau_2}{3}(k_2^2 H_2 + f_h k_2 v_2^2) k_1 H_1 + 2\frac{\tau_3}{3}(k_1 H_1 k_3^2 H_3) - 2(\lambda + \overline{\beta}_2 + \overline{\beta}_3) k_1^2 H_1, \tag{14}$$

$$\partial_t H_2 = -2\frac{\tau_2}{3}(k_2^2 H_2 + f_h k_2 v_2^2) k_1 H_1 - 2\frac{\tau_3}{3}(k_2 H_2 k_3^2 H_3 f_u) + 2\overline{\beta}_2 k_1^2 H_1 - 2 g_u (\beta_3)_2 k_2^2 H_2 - 2\lambda k_2^2 H_2, \tag{15}$$

$$\partial_t H_3 = 2\frac{\tau_3}{3}(k_2 H_2 k_3^2 H_3 f_u) - 2\frac{\tau_3}{3}(k_1 H_1 k_3^2 H_3) + 2\overline{\beta}_3 k_1^2 H_1 + 2 g_u (\beta_3)_2 k_2^2 H_2 - 2\lambda k_3^2 H_3, \tag{16}$$

and

$$\partial_t H_4 = -2\lambda k_4^2 H_4. \tag{17}$$

The last equation is decoupled from the others, and represents decay. Thus in present approximation scheme, where correlations between different scales vanish and $k_4 = k_\lambda \geq k_3$ there is no helicity exchange with the resistive scale. Equation (17) can then be subsequently ignored.

The third and fifth terms of (15) and the second and fifth terms of (16) involve the quantities f_u and g_u. These are positive quantities and they come from the subtlety in dotting the second and third terms of (13) with $\mathbf{b}_2$: dotting the third term of (13) with $\mathbf{b}_2$ gives the term $\propto \langle(\beta_3)_2\mathbf{j}_2\cdot\mathbf{b}_2\rangle_{vol} = \langle\beta_3\rangle_{vol}\langle\frac{(\beta_3)_2}{\langle\beta_3\rangle_{vol}}\mathbf{j}_2\cdot\mathbf{b}_2\rangle_{vol} = \langle\beta_3\rangle_{vol} = \langle\frac{(\beta_3)_2}{\langle\beta_3\rangle_{vol}}\mathbf{j}_2\cdot\mathbf{b}_2\rangle_{vol} = \langle\beta_3\rangle_{vol}g_u k_2^2 H_2$, where g_u accounts for the deviation of $\frac{(\beta_3)_2}{\langle\beta_3\rangle_{vol}}$ from unity, and I also assume that $\overline{\beta}_2 = \langle\beta_2\rangle_{vol}$ and $\overline{\beta}_3 = \langle\beta_3\rangle_{vol}$. Similarly, dotting the second term of (13) with $\mathbf{b}_2$ and averaging gives a term $\propto \langle(\mathbf{j}_3\cdot\mathbf{b}_3)_2\mathbf{b}_2^2\rangle_{vol} = \langle\mathbf{j}_3\cdot\mathbf{b}_3\rangle_{vol}\langle\frac{(\mathbf{j}_3\cdot\mathbf{b}_3)_2}{\langle\mathbf{j}_3\cdot\mathbf{b}_3\rangle_{vol}}\mathbf{b}_2^2\rangle_{vol} \equiv -\langle\mathbf{j}_3\cdot\mathbf{b}_3\rangle_{vol}f_u k_2 H_2$ so that f_u accounts for both the fractional helicity at the k_2 scale and the deviation of the ratio $\frac{(\mathbf{j}_3\cdot\mathbf{b}_3)_2}{\langle\mathbf{j}_3\cdot\mathbf{b}_3\rangle_{vol}}$ from unity. Note that unlike b_2^2, b_3^2 does not enter these equations so that even if there is a large pile-up in magnetic energy at k_3 initially, only its force-free component couples into the above equations.

To write equations (14), (15), and (16) in dimensionless form, I define $h_1 \equiv H_1(k_2/v_2^2)$, $h_2 \equiv H_2(k_2/v_2^2)$, $h_3 \equiv H_3(k_2/v_2^2)$, $R_M \equiv v_2/\lambda k_2$, $\tau \equiv t v_2 k_2$, use $\overline{\mathbf{v}_2\cdot\nabla\times\mathbf{v}_2} = -f_h k_2 v_2^2$. I assume that $\overline{\beta}_2 = q(h_1)v_2/3k_2$ and $\overline{\beta}_3 = q(h_1)v_3/3k_3$, where $q(h_1)$ is a quenching function for the diffusivity that I take to be $q(h_1) = (1+k_1 h_1/k_2)^{-1}$. The main points of the present study are insensitive to the form of q, but pinning it down requires more study. I also use a Kolmogorov velocity spectrum so that $v_3 = (k_2/k_3)^{1/3}v_2$ and $\tau_3 = (k_2/k_3)^{2/3}\tau_2$. The result is

$$\partial_\tau h_1 = \tfrac{2}{3}\left(f_h + h_2 + \left(\tfrac{k_3}{k_2}\right)^{\frac{4}{3}} h_3\right)\tfrac{k_1}{k_2}h_1 - 2\left(\tfrac{q(h_1)}{3} + \tfrac{q(h_1)}{3}\left(\tfrac{k_2}{k_3}\right)^{\frac{4}{3}} + \tfrac{1}{R_M}\right)\left(\tfrac{k_1}{k_2}\right)^2 h_1, \tag{18}$$

$$\partial_\tau h_2 = \tfrac{-2}{3}\left(\tfrac{k_3}{k_2}\right)^{\frac{4}{3}} f_u h_3 h_2 - \tfrac{2}{3}\left(f_h + h_2\right)\tfrac{k_1}{k_2}h_1 + \tfrac{2q(h_1)}{3}\left(\tfrac{k_1}{k_2}\right)^2 h_1 - 2\left(\tfrac{q(h_1)}{3}g_u\left(\tfrac{k_2}{k_3}\right)^{\frac{4}{3}} + \tfrac{1}{R_M}\right)h_2, \tag{19}$$

and

$$\partial_\tau h_3 = \tfrac{2}{3}\left(\tfrac{k_3}{k_2}\right)^{\frac{4}{3}} f_u h_3 h_2 - \tfrac{2}{3}\left(\tfrac{k_3}{k_2}\right)^{\frac{4}{3}}\left(\tfrac{k_1}{k_2}\right)h_3 h_1 + \tfrac{2q(h_1)}{3}\left(\tfrac{k_2}{k_3}\right)^{\frac{4}{3}}\left(\tfrac{k_1}{k_2}\right)^2 h_1 + \tfrac{2q(h_1)}{3}g_u\left(\tfrac{k_2}{k_3}\right)^{\frac{4}{3}} h_2 - \tfrac{2}{R_M}\left(\tfrac{k_3}{k_2}\right)^2 h_3. \tag{20}$$

These equations are to be solved for h_1, h_2 and h_3 as a function of time. They can model a four-scale nonlinear dynamo theory in which helicity decays at the resistive scale but is allowed to transfer between the system scale, the forcing scale, and the viscous scale. We will compare the solutions with those of the two-scale system of equations:

$$\partial_\tau h_1 = \frac{2}{3}\left(f_h + h_2\right)\frac{k_1}{k_2}h_1 - 2\left(\frac{q(h_1)}{3} + \frac{1}{R_M}\right)\left(\frac{k_1}{k_2}\right)^2 h_1 \tag{21}$$

$$\partial_\tau h_2 = -\frac{2}{3}\left(f_h + h_2\right)\frac{k_1}{k_2}h_1 + \frac{2q(h_1)}{3}\left(\frac{k_1}{k_2}\right)^2 h_1 - \frac{2}{R_M}h_2 \tag{22}$$

obtained from (14), (15), and (16) by setting $H_3 = 0$ and $\beta_3 = 0$ and then non-dimensionalizing. Equations (21) and (22) are essentially the same as those solved in Field & Blackman (2002) and which emerged as the specific limit of the strong damping approximation in the generalized two-scale theory of Blackman & Field (2002). Using the doublet (21) and (22) of equations rather than the triplet of equations which also includes $\partial_t \overline{\boldsymbol{\mathcal{E}}}$ cannot capture possible oscillations in the early time growth of h_1. (Related oscillations were identifed in simulations by Stribling, Matthaeus, Ghosh 1994 when a uniform field was imposed in their periodic box.) These can be accounted for only when one allows for a variation in the damping time in the $\partial \overline{\boldsymbol{\mathcal{E}}}_2$ equation. Similarly, the use of the four equations (14-17) rather than 6 equations that would result from also including equations for $\partial_t \overline{\boldsymbol{\mathcal{E}}}_2$ and $\partial_t \overline{\boldsymbol{\mathcal{E}}}_3$ is similarly restrictive in the present context. We leave the necessary generalizations for future work.

3. Discussion of Solutions

The critical helicity for growth of h_1 to beat diffusion is $f_h \gtrsim k_1/k_2$. For f_h below this value, h_1, h_2, and h_3 all decay. This is consistent with numerical simulations of Maron & Blackman (2002). Below we focus on the case $f_h = 1$ to emphasize the main ideas. We also assume $g_u = f_u = 1$ to simplify the discussion, and a seed of $h_1 \sim 0.001$. The associated solutions of (18), (19), and (20) will be discussed along with the comparison to solutions of (21) and (22).

3.1. Large scale field growth in the kinematic regime

By kinematic regime we mean the growth regime in which h_1 grows independently of R_M. This is essentially the time for h_2 to approach $-f_h$ (see (18)). At early times, before resistivity is important, $h_2 \sim -h_1$, so we can estimate the duration of the kinematic regime by determining the time at which $h_1 \sim f_h$. We have, from (18),

$$t_{kin} \sim 3(k_2/k_1)\mathrm{Ln}(f_h/h_1(0)), \tag{23}$$

which is ~ 100 for $f_h = 1$, $k_2/k_1 = 5$ and $h_1(0) = 0.001$, as used herein.

A careful look at (18), (19), and (20) shows that for a small seed h_1 and $h_3(0) \lesssim f_h(k_2/k_3)^{4/3}$, the kinetic helicity drives the growth of h_1 and the growth of the oppositely signed h_2. (If $h_3(0)$ exceeds the above critical value then h_1 and h_3 initially decay until h_3 falls below that value, after which h_1 starts to grow.) The growth of h_2 also supplies, from diffusion, a growth of h_3 from the 5th term in (20). For $k_2 < k_3 << k_\lambda$,

the value of h_1 at the end of the kinematic phase in the four-scale approach saturates at a slightly smaller value of h_1 than for the two-scale case. The slight difference between the two curves can be explained by ignoring diffusion and dissipation terms (those containing q and R_M) in (18), (19), and (20) and assuming a quasi-steady state. Setting time derivatives to zero in (18), (19), and (20) then gives a system of three equations:

$$(1 - k_1/k_2 + h_2 + (k_3/k_2)^{4/3} h_3) \simeq 0, \tag{24}$$

$$h_2 h_3 = h_1 h_3 (k_1/k_2) - h_2 (k_2/k_3)^{8/3} \sim -h_2 (k_2/k_3)^{8/3} \tag{25}$$

and

$$h_1 + h_2 + h_3 \simeq 0, \tag{26}$$

where we have assumed $h_2 >> h_1 k_1/k_2$ anticipating that h_3 is small. The solution is $h_1 \simeq 1 - k_1/k_2 - (k_2/k_3)^{4/3} + (k_2/k_3)^{8/3}$, $h_2 \simeq -1 + (k_2/k_3)^{4/3} + k_1/k_2$, and $h_3 \simeq -(k_2/k_3)^{8/3}$. Thus no matter what $k_3 << k_\lambda$ is chosen, h_1 is only slightly depleted from $h_1 \sim 1 - k_1/k_2$, the value h_1 attains in the kinematic regime for the two-scale approach. For $k_3 \to k_2$ in (24), (25), and (26) $h_1 \to 1 - k_1/k_2$. Also, for $k_3 >> 1$, $h_1 \to 1 - k_1/k_2$. The correction to h_1 is maximized for $k_2/k_3 = 0.6$ at which the deficit is about 25%. In short, $h_1 \to 1$, as in the kinematic regime here just as in the two-scale approach. For $k_3 = 30$ and $R_M = 9000$, these results are seen in the bottom pair of curves in the upper left plot of Fig. 1, where the bold line is the h_1 solution of the two-scale system (21) and (22) and the thin line is h_1 for the four-scale system. The top set of curves in the same plot shows the $k_3 = 30$ and $R_M = 900$ case. There, h_3 first grows as in the previous case, but drains more quickly from resistivity. Growth of h_1 then more closely mimics the kinematic evolution of h_1 in the two-scale approach at very early times.

That $h_3 \simeq -(k_2/k_3)^{8/3}$ at the end of the kinematic regime shows that as k_3 increases for fixed k_2, h_3 decreases. This is demonstrated in the bottom left plot of Fig. 1 which shows the growth of h_1 for $R_M = 100$ and $R_M = 2 \times 10^4$ and $k_3 = 160$. There, even the high R_M four-scale solution matches the two-scale approach exactly.

3.2. Rapid migration of the small scale peak to the forcing scale in the kinematic regime

An important implication of including the scale k_3 can seen by comparing the ratio of the magnetic energy and current helicity at scales k_2 and k_3 to those of k_1, as a function of time. This is shown in Figs. 2, 3 and 4 for different cases. In general, the current helicity and magnetic energy are dominated by the k_3 scale at early times. These quantities are related to the magnetic helicity by factors of k^2 and k respectively. The diffusion of h_2 into

h_3 grows enough h_3 for $k_3 h_3$ and $k_3^2 h_3$ to exceed the respective values at k_1 and k_2 initially. The early time dominance of the k_3 quantities is enhanced when there is an initial seed of h_3, as seen by comparing Figs. 3 and 4. For a Kolmogorov velocity spectrum however, the small scale current helicity and associated magnetic energy end up being dominated by the forcing scale before t_{kin}: as discussed below (26), the maximum h_3 at the end of the kinematic regime is $h_3 \sim -(k_2/k_3)^{8/3}$ so that the ratio of current helicity at k_3 to that at k_2 is then is $(k_3/k_2)^2(h_3/h_2) \sim (k_2/k_3)^{2/3} << 1$, since $h_2 \sim 1$.

It is interesting to asses whether the times for crossover of small scale dominance from k_3 to k_2 quantities depends on magnetic Reynolds number. The answer is that for large R_M it does not, but for low R_M it does. One can be misled if applying the low R_M results to large R_M. To see this more explicitly, first note that the location of the crossovers for the case of Fig. 3 does depend on R_M: The lower the R_M the earlier the crossovers. However, for large R_M, the location of the crossover asymptotes to an R_M independent value. It has been checked that the location of the crossovers for $R_M = 9000$ in Fig. 3 is indistinguishable for the location of the cross over for any higher R_M, keeping all other parameters fixed. This latter result is more directly seen in the comparisons of the top and bottom rows of Figs. 3 and 4. There, the top rows in both cases correspond to a comparison between $R_M = 100$ and $R_M = 2 \times 10^4$ for $k_3 = 160$. The bottom rows correspond to a comparison between $R_M = 100$ and $R_M = 2 \times 10^5$ for $k_3 = 160$. The locations of the cross over for the $R_M = 2 \times 10^4$ and $R_M = 2 \times 10^5$ cases are indistinguishable.

Note that the case of $k_3 = 160$ and $R_M = 100$ for $k_2 = 5$ is the case of $k_3 \simeq k_\lambda \simeq k_\nu$ for Kolmogorov turbulence, in other words, $Pr_M \simeq 1$. This follows because choosing $R_M = 100$ for $k_3 = 160$ also corresponds to choosing $(k_3/k_2) = R^{3/4} \simeq 100$, where R is the hydrodynamic Reynolds number and where k_3 is taken to be the viscous wavenumber. The power 3/4 follows from the Kolmogorov spectrum. This can be distinguished from any $R_M >> 100$ for fixed k_3, which, in turn, represents $Pr_M >> 1$.

Thus, restating the results of this section in terms of Pr_M, we can say that for the $Pr_M = 1$ case the crossover time for the current helicity at k_3 to deplete below that at k_2 is earlier than for the $Pr_M >> 1$ case in which $k_3 << k_\lambda$. This is expected, since the resistivity is not effective at dissipating k_3 for $Pr_M >> 1$. At large R_M for fixed $k_3 = k_\nu$ (or $Pr_M >> 1$), the crossover is the result of the dynamical depletion of h_3 from the first two terms on the right of (20), and becomes independent of R_M or Pr_M.

3.3. Saturation: the doubly maximal inverse transfer state

The growth term for h_3 at early times is the fifth term in (20), but eventually this is offset by the fourth term, after which the only remaining terms for h_3 are resistive and inverse transfer loss terms. Thus, as we have seen, h_3 eventually decays, whilst h_2 continues to grow. The latter takes over the role of compensating negative helicity, and the saturation proceeds exactly in the two-scale approach: positive helicity at h_1 and negative helicity h_2 at the forcing scale. This is demonstrated in the right column of Fig. 1 where the late time evolution of the two-scale and four-scale approaches are seen to be indistinguishable for all R_M. Accordingly, at late times, the current helicity at k_2 asymptotes to equal that at k_1, just as in the two-scale approach (Brandenburg 2001; Field & Blackman 2002; Blackman & Field 2002).

The features of the four-scale model discussed herein can be used as an aid to understand the full saturated spectrum of the helical dynamo both above and below the forcing scale. Consider $k_L \leq k_1 < k_f \leq k_2 < k_3 \leq k_\nu$, where k_L is the wavenumber of the largest scale available, k_f is the forcing scale and k_ν is the viscous scale and we allow k_1, k_2, k_3 to take on intermediate values. The time for the spectrum to evolve depends on the ratios k_L/k_f and k_f/k_ν, but the qualitative evolution can be understood simply. At early times, a seed spectrum forced with negative kinetic helicity with $f_h > k_1/k_f$, can grow positive magnetic helicity at k_1. (For $f_h = 1$ the maximum growth of the large scale magnetic helicity initially occurs at $k_1 \simeq k_2/2$.) The magnetic helicity will inverse transfer from $k_1 > k_L$ to successively smaller k, eventually all the way to k_L. The k_L will continue to accumulate the bulk of the positive magnetic helicity until saturation. This happens by direct analogy to the sub-forcing scale dynamics discussed earlier. There the negative magnetic helicity initially grows fastest on the scale k_ν before loss terms eventually win on that scale, and the negative magnetic helicity transfers upward to larger scales, eventually reaching the forcing scale where the bulk of the negative magnetic helicity collects. *The positive and negative magnetic helicities thus migrate to their largest available scales.* The negative helicity cannot grow at any k significantly less than k_f since the growth rate for positive magnetic helicity is positive for lower k. The overall picture just outlined for saturation seems to be consistent with simulations of Brandenburg (2001) and Maron & Blackman (2002).

Note that the larger the scale, the less important the resistive terms in draining the helicities from those scales. The dominant loss terms for $k << k_\lambda$ are the inverse transfer terms, not resistive terms. The threshold magnetic helicity at a given scale for the inverse transfer loss to dominate its gain from diffusion of magnetic helicity from larger scales, increases with decreasing k. Thus, larger scales take longer to inverse transfer their

magnetic helicity. For the positive helicity above the forcing scale, this means that the k_L scale takes the longest to grow to its maximum, and for the negative helicity, k_f takes the longest to grow to its maximum. The final state can be described as a state of "doubly maximal inverse transfer."

3.4. Implications and comparison to fractionally helical dynamo spectra

Maron & Blackman (2002) showed that as f_h exceeds k_L/k_f and approaches 1 for $Pr_M > 1$, the saturated magnetic energy spectrum changes from peaking on the resistive scale to peaking on two scales, with one peak at the forcing scale and one at the system scale. (Their $f_h = 1$ results matched Brandenburg 2001.) For $f_h > k_L/k_f$, $f_h(k_L/k_f)$ times the equipartition energy ends up in magnetic energy at the the k_1 scale after the kinematic regime. At saturation, $f_h k_f/k_L$ of the equipartition energy ends up at k_L.

The fraction of small scale magnetic energy associated with the helicity dynamics is also determined by f_h. Whatever the dynamics of the nonhelical magnetic energy spectrum, the helical fraction of the magnetic spectrum seems to be explicable by the independent dynamics discussed above, suggesting that the helical and nonhelical parts of the spectrum are rather decoupled. Recall that the nonhelical magnetic energies on the k_3 and k_λ scales do not enter the theory, only that on the k_2 scale (see the discussion between equations (17) and (18)). In the present theory, the expected helical fraction of the small scale magnetic energy that follows the helicity dynamo dynamics is given simply by f_h. This follows because the small scale current helicity in saturation is $f_h v^2 k_2 \sim \langle \mathbf{b} \cdot \nabla \times \mathbf{b} \rangle$ and since $\langle \mathbf{b}^2 \rangle \sim \langle \mathbf{v}^2 \rangle$ in saturation, we have the associated helical magnetic energy fraction $= f_h$. If we include the nonhelical component of the magnetic energy, then f_h is a lower limit to the fraction of the total small scale magnetic energy that winds up at the forcing scale.

4. Conclusions

A four scale nonlinear magnetic dynamo theory was presented using the approximation that correlations of mixed scales are assumed to vanish. The goal was to develop a simple theory that sheds light on the evolution of the full magnetic spectrum for the helical dynamo and show how the presence of kinetic helicity influences the spectrum both above and below the dominant scale of the turbulent kinetic energy. The velocity spectrum was assumed to be Kolmogorov, with kinetic helicity input only at the forcing scale. The results of the simple theory are consistent with existing numerical simulations and make additional

predictions which can be tested. The theory includes the dynamical backreaction of the growing magnetic field on the turbulence driving the field growth.

The growth of the large scale field in the four scale theory is consistent with that predicted in the two-scale theory (Field & Blackman (2002); Brandenburg & Blackman (2002); Blackman & Field (2002)) at late times but previous simulations do not have enough resolution to test the dynamics of the kinematic regime and so higher resolution simulations will be needed. The four-scale theory herein predicts that as the large helical scale field grows, the small scale helical field of the opposite sign and its associated current and magnetic helicity will first grow at the smallest scales where both $\mathbf{v}$ and $\mathbf{b}$ are finite (for $Pr_{\geq}1$, this is the viscous scale). This cannot be seen in a two-scale approach, since there the system scale and forcing scales are the only ones present. The source of helical field for the very smallest scales is diffusion from above. These very small (viscous) scale helical fields drain by inverse transfer, and the helical magnetic energy below the forcing scale peaks at successively larger scales, arriving at the forcing scale before t_{kin}. If the viscous scale is much larger than the resistive scale, then resistivity plays little role in this process; the process is independent of R_M for large R_M. At t_{kin} the growth of both the large and small scale helical fields proceed exactly as in the two-scale theory: large scale current and magnetic helicities are primarily carried by k_1, and the oppositely signed small scale quantities at scale k_2.

That high resolution simulations are needed to test the kinematic regime also means that they are need for testing the assumption made above Eqn. (7). If future simulations for $Pr_M >> 1$ show that the current helicity piles up at the resistive scale rather than the viscous scale at very early times, this would suggest that the approximation that correlations of mixed scales vanish would have to be revised, since it is only such mixed correlations which can grow helicity on the resistive scale. In the present, four-scale theory, the helical magnetic energy on the resistive scale decays, and the nonhelical component is decoupled from the helical component. I emphasize that the model presented herein is a simplified theory, meant to guide physical understanding of helical MHD turbulence. It must be subject to further testing.

The larger the fractional kinetic helicity f_h, the more the overall magnetic spectrum behaves like its helical component. If the nonhelical component prefers to pile-up at small scales, the helical component will provide at least some fraction that wants to be doubly peaked at the forcing and system scales. It is thus important to emphasize that that driving turbulence with kinetic helicity on a scale k_2 affects the shape of the overall helical magnetic energy spectrum and thus that of the overall magnetic energy spectrum above and below the forcing scale.

Many thanks to G. Field, A. Brandenburg, B. Chandran, H. Ji, R. Kulsrud and J. Maron for discussions. DOE grant DE-FG02-00ER54600 is acknowledged. Thanks to the Department of Astrophysical Sciences and the Plasma Physics Lab at Princeton for hospitality during a sabbatical.

REFERENCES

Balbus, S.A. & Hawley, J.F., 1991, ApJ, 376, 214,

Balbus, S.A. & Hawley, J.F., 1998, Rev Mod Physics, 72 1,

Beck, R., Brandenburg, A., Moss, D., Shukurov, A., & Sokoloff, D. 1996, ARAA, 34, 155

Bhattacharjee, A., & Yuan, Y., 1995, ApJ, 449, 739

Bellan, P.M. 2000, *Spheromaks*, (London: Imperial College Press)

Berger, M.A., & Field, G.B., 1984, J. Fluid Mech., 147, 133

Blackman, E.G. & Field, G.B., 2000, ApJ, 534, 984

Blackman, E.G. & Field, G.B,, 2002, Phys. Rev. Lett. 89, 265007

Blackman, E. G. & Brandenburg, A. 2002, ApJ, 579, 359

Blackman E.G., 2002, To appear in *Turbulence and Magnetic Fields in Astrophysics* eds. E. Falgarone and T. Passot, Springer Lecture Notes in Physics, astro-ph/0205002

Blackman, E. G. 2002, to appear in proceedings of the 1st Niels Bohr Summer Institute: "Beaming and Jets in Gamma-Ray Bursts", Copenhagen, Aug 2002, edited by R. Ouyed, J. Hjorth and . Nordlund, astro-ph/0211187,

Blackman, E.G., 2003, in proceedings of the 1st Niels Bohr Summer Institute: "Beaming and Jets in Gamma-Ray Bursts", Copenhagen, Aug 2002, edited by R. Ouyed, J. Hjorth & . Nordlund, astro-ph/0211187

Brandenburg, A., Nordlund, A., Stein, R. F., & Torkelsson, U. 1995, ApJ, 446, 741

Stone, J. M., Hawley, J. F., Gammie, C. F., & Balbus, S. A. 1996, ApJ, 463, 656

Brandenburg, A. & Donner, K.J., 1997, MNRAS 288 L29,

Brandenburg, A., 2001, ApJ, 550, 824

Brandenburg, A. 2002 to appear in *Turbulence and Magnetic Fields in Astrophysics*, eds. E. Falgarone and T. Passot, Springer Lecture Notes in Physics (astro-ph/0207394)

Brandenburg, A., Dobler, W., & Subramanian, K. 2002, Astronomische Nachrichten, 323, 99

Cattaneo, F. & Hughes, D.W., 1996, Phys. Rev. E., 54, 4532

Cattaneo F., Hughes, D.W. & Thelen, J.C., 2002, JFM, 456, 219

Field G.B., & Blackman, E.G., 2002, ApJ, 572, 685

Field, G.B., Blackman, E.G., & Chou, H., 1999, ApJ, 513, 638

Gruzinov, A.V., & Diamond, P.H., 1995, Phys. of Plasmas, 2, 1941

Haugen, N.E.L, Branendburg A., Dobler W., 2003, submitted to PRL, astro-ph/0303372.

Hawley, J.F., Gammie, C.F, 1995, & Balbus, S.A., ApJ 440, 742

Hawley, J.F., Gammie, C.F, 1995, & Balbus, S.A., ApJ 464, 690

Cho, J., Lazarian, A., & Vishniac, E. T. 2002, ApJL, 566, L49

Ji, H., 1999, Phys. Rev. Lett., 83, 3198

Ji H., & Prager S.C., in press Magnetohydrodynamics, astro-ph/0110352 (2002)

Kida, S., Yanase, S., & Mizushima, J. 1991, Physics of Fluids, 3, 457,

Kleeorin, N.I., & Ruzmaikin, A.A., 1982 Magnetohydrodynamics, 18, 116

Kleeorin, N.I., Rogachevskii, I., Ruzmaikin, A., A&A, 1995, 297, L59

Krause, F. & Rädler, K.-H. (1980) *Mean-Field Magnetohydrodynamics and Dynamo Theory* (New York: Pergamon Press)

Kulsrud, R.M. & Anderson, S.W., 1992, ApJ, 396, 606

Maron, J. & Blackman, E.G., 2002, ApJ, 566, L41

Maron, J. & Goldreich, P. 2001, ApJ, 554, 1175

Maron, J. & Cowley, S., 2002, submitted to ApJ, astro-ph/0111008,

Ortolani, S. & Schnack, D.D., 1993, "Magnetohydrodynamics of Plasma Relaxation" (Singapore: World Scientific)

Moffatt, H. K. 1978, *Magnetic Field Generation in Electronically Conducting Fluids* (Cambridge: Cambridge University Press)

Parker, E. N., 1955, ApJ, 122, 293

Parker, E. N., 1979, *Cosmical Magnetic Fields* (Oxford: Clarendon Press).

Piddington, J.H. 1981 *Cosmical Electrodynamics*, (Malbar: Krieger Press)

Pouquet, A., Frisch, U., & Leorat, J., 1976, J.Fluid Mech., 77, 321

Rädler, K.-H. Astron. Nachr., 1980, 301, 101

Ruzmaikin, A., Shukurov, A.M., Sokoloff, D.D., 1988, *Magnetic Fields of Galaxies*, (Dodrecht: Kluwer Press).

Schekochihin, A., Cowley, S., Maron, J., Malyshkin, L., 2002a, Phys Rev. E., 65, 6305

Schekochihin, A.A., Cowley, S.C., Hammett, G.W., Maron J.L., McWilliams, J.C. 2002b, New J. Phys., 4, 84

Steenbeck, M., Krause, F., & Rädler, K. H. 1966, Z. Naturoforsch, 21a, 369

Stribling, T., Matthaeus W.M., Ghosh, S., 1994, J. Geophys. Res., 99, 2567

Vainshtein S.I. & Cattaneo F., 1992, ApJ, 393, 165

Woltjer, L., 1958, Proc. Nat. Acad. Sci., 44, 489

Zeldovich Ya. B. , Ruzmaikin A.A., and Sokoloff D.D., 1983, *Magnetic Fields in Astrophysics*, (New York: Gordon and Breach)

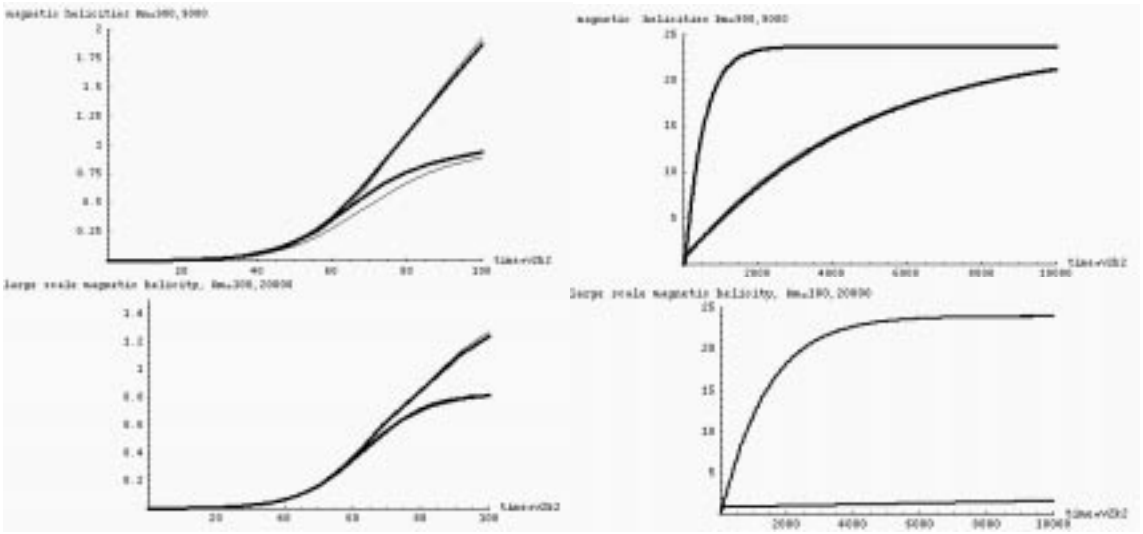

Figure 1: The magnetic helicity, h_1, for the four-scale approach (thin lines) and the two-scale approach (thick lines). The left column of plots is for early times and the right column is for a broader time range. For the top row, $k_1 = 1$, $k_2 = 5$, $k_3 = 30$, and $R_M = 900$ (top pair of curves) $R_M = 9000$ (bottom pair of curves). For the bottom row, $k_1 = 1$, $k_2 = 5$, $k_3 = 160$, and $R_M = 100$ (top pair of curves) $R_M = 2 \times 10^4$ (bottom pair of curves). Note that the two-scale and four-scale approaches are largely indistinguishable in all but the upper left plot (see text). (The high R_M curve in the lower right will eventually saturate at the same value $h_1 = (k_2/k_1)^2$ as the low R_M case but at much later times and thus undershoots the top curve for the plotted time range.)

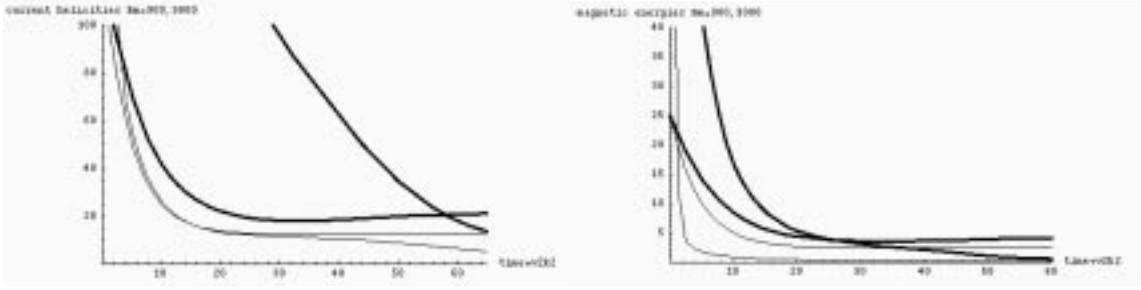

Figure 2: The absolute magnitude of the current helicity ratios $|k_2^2 h_2/k_1^2 h_1|$ and $|k_3^2 h_2/k_1^2 h_1|$, and helical magnetic energy ratios $|k_2 h_2/k_1 h_1|$ and $|k_2 h_2/k_1 h_1|$ assuming an initial seed of $h_2(0) = h_3(0) = -h_1(0)/2 = 0.0005$. Here $R_M = 900$ (thin lined curves) $R_M = 9000$ (thick lined curves) for $k_1 = 1$, $k_2 = 5$, $k_3 = 30$. In each plot, and for both values of R_M, the quantities at k_3 dominate at early times, and then become subdominant to the values at k_2 at later times. The location of the crossover is earlier for $R_M = 900$ because the resistive scale is closer to the scale k_3; resistivity is more effective at early times in draining the current helicity and magnetic energy at k_3 than in the $R_M = 9000$ case.

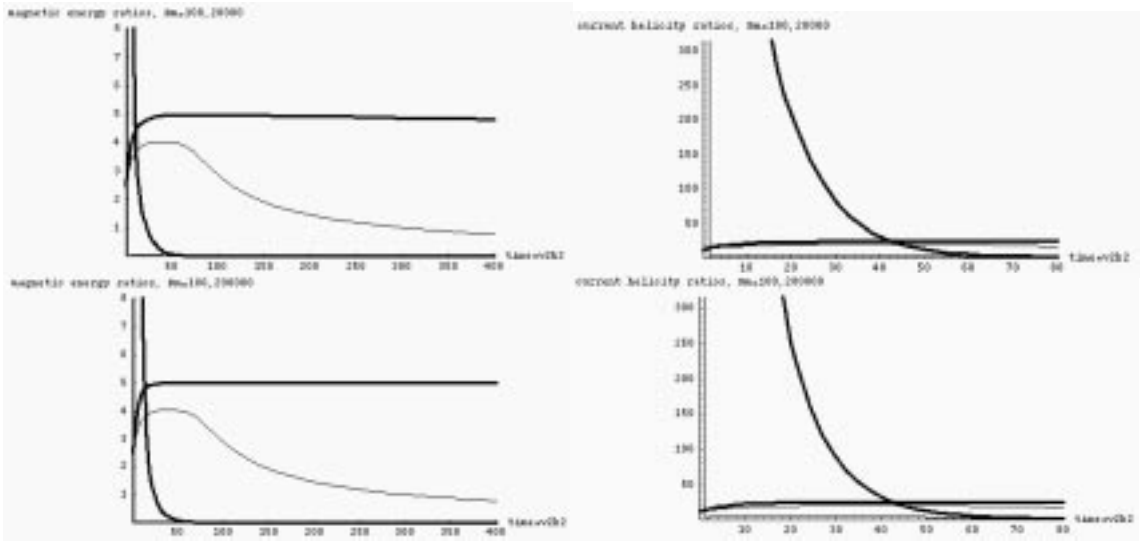

Figure 3: The absolute magnitude of the current helicity ratios $|k_2^2 h_2/k_1^2 h_1|$ and $|k_3^2 h_2/k_1^2 h_1|$, and helical magnetic energy ratios $|k_2 h_2/k_1 h_1|$ and $|k_2 h_2/k_1 h_1|$ assuming an initial seed of $h_2(0) = h_3(0) = -h_1(0)/2 = 0.0005$. for $k_1 = 1$, $k_2 = 5$, $k_3 = 160$. Top row has plots for $R_M = 100$ (thin lined curves) and $R_M = 2 \times 10^4$ (thick lined curves), and bottom row has plots for $R_M = 100$ (thin lined curves) and $R_M = 2 \times 10^5$ (thick lined curves). In each plot, the quantities at k_3 dominate at early times, but then become subdominant to the values at k_2 at later times. The magnetic energy plot is shown for a broader time range. The location of the crossover for the large R_M cases of 2×10^4 and 2×10^5 is independent of R_M: the crossovers occur for the thick pairs of lines at the same time in the top and bottom rows. The crossover occurs much earlier for $R_M = 100$ because the resistive wavenumber is closser to k_3 and thus resistivity is more effective at early times in draining the current helicity and magnetic energy at k_3 than in the larger R_M cases. For the current helicity, the cross over for $R_M = 100$ occurs so early that it is not visible on the graph. Before the end of the kinematic regime ($t \lesssim 100$), the crossovers are complete and k_2 emerges as the dominant small scale. Since $k_3 = 160$ here, $R_M = 100$ corresponds to $Pr_M \simeq 1$

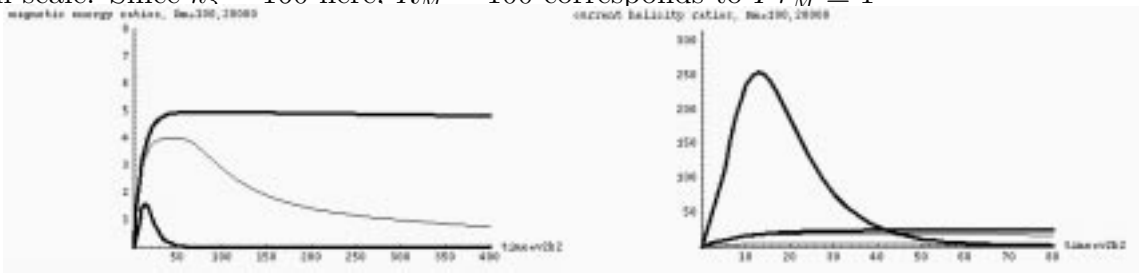

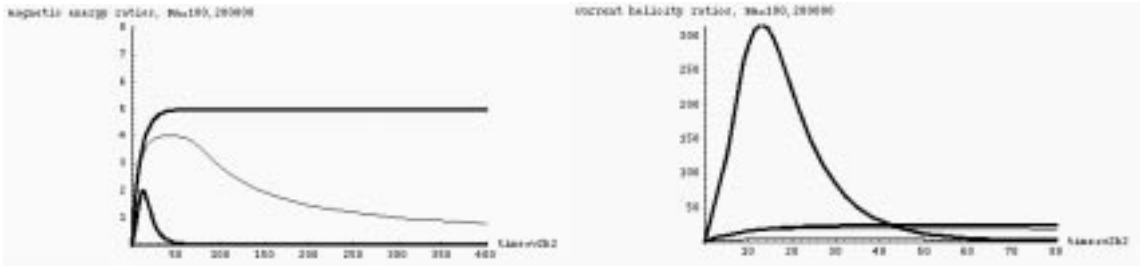

Figure 4: Same as Figure 3, but with $h_1(0) = 0.001$ and $h_2(0) = h_3(0) = 0$. Note the initial rise of the current helicity and magnetic energy at k_3 but then again the dominance of the k_2 quantities before the end of the kinematic regime $t_{kin} = 100$